the FEBS Journal

The starch-binding capacity of the noncatalytic SBD2 region and the interaction between the N- and C-terminal domains are involved in the modulation of the activity of starch synthase III from *Arabidopsis thaliana*

Enzymes and catalysis

Nahuel Z. Wayllace[1,2], Hugo A. Valdez[1], Rodolfo A. Ugalde[1,†], Maria V. Busi[1,2] and Diego F. Gomez-Casati[1,2]

1 Instituto de Investigaciones Biotecnológicas-Instituto Tecnológico de Chascomús, Argentina
2 Centro de Estudios Fotosintéticos y Bioquímicos, Universidad Nacional de Rosario, Argentina

Keywords
Arabidopsis; enzyme regulation; protein interaction; starch synthase; starch-binding domain

Correspondence
D. F. Gomez-Casati, Centro de Estudios Fotosintéticos y Bioquímicos (CEFOBI-CONICET), Universidad Nacional de Rosario, Suipacha 531, 2000, Rosario, Argentina
Fax: +54 341 437 0044
Tel: +54 341 437 1955
E-mail: gomezcasati@cefobi-conicet.gov.ar

†Deceased

(Received 14 September 2009, revised 10 November 2009, accepted 13 November 2009)

doi:10.1111/j.1742-4658.2009.07495.x

Starch synthase III from *Arabidopsis thaliana* contains an N-terminal region, including three in-tandem starch-binding domains, followed by a C-terminal catalytic domain. We have reported previously that starch-binding domains may be involved in the regulation of starch synthase III function. In this work, we analyzed the existence of protein interactions between both domains using pull-down assays, far western blotting and co-expression of the full and truncated starch-binding domains with the catalytic domain. Pull-down assays and co-purification analysis showed that the D(316–344) and D(495–535) regions in the D2 and D3 domains, respectively, but not the individual starch-binding domains, are involved in the interaction with the catalytic domain. We also determined that the residues W366 and Y394 in the D2 domain are important in starch binding. Moreover, the co-purified catalytic domain plus site-directed mutants of the D123 protein lacking these aromatic residues showed that W366 was key to the apparent affinity for the polysaccharide substrate of starch synthase III, whereas either of these amino acid residues altered ADP-glucose kinetics. In addition, the analysis of full-length and truncated proteins showed an almost complete restoration of the apparent affinity for the substrates and V_{max} of starch synthase III. The results presented here suggest that the interaction of the N-terminal starch-binding domains, particularly the D(316–344) and D(495–535) regions, with the catalytic domains, as well as the full integrity of the starch-binding capacity of the D2 domain, are involved in the modulation of starch synthase III activity.

Structured digital abstract

- MINT-7299461: *SSIII* (uniprotkb:Q9SAA5) *binds* (MI:0407) to *SSIII* (uniprotkb:Q9SAA5) by *far western blotting* (MI:0047)
- MINT-7299411, MINT-7299429, MINT-7299445: *SSIII* (uniprotkb:Q9SAA5) *binds* (MI:0407) to *SSIII* (uniprotkb:Q9SAA5) by *pull down* (MI:0096)

Abbreviations
ADPGlc PPase, ADP-glucose pyrophosphorylase; ADPGlc, ADP-glucose; CBM, carbohydrate-binding module; CD, catalytic domain; GA-1, glucoamylase-1; GB, granule-bound; GS, glycogen synthase; SBD, starch-binding domain; SS, starch synthase.

Introduction

Starch plays a central role as the major carbohydrate storage form and source of chemical energy in plants. This polysaccharide is composed of amylose, which is predominantly a linear α-1,4-glucan chain, and amylopectin, a highly branched α-1,4-α-1,6-glucan. Starch synthesis involves a series of steps catalyzed by ADP-glucose pyrophosphorylase (ADPGlc PPase, EC 2.7.7.27), starch synthase (SS, EC 2.4.1.21) and branching enzyme (EC 2.4.1.18) [1–4]. Whereas the production of ADPGlc via ADPGlc PPase is the first committed step in starch biosynthesis, SS catalyzes the elongation of α-1,4-glucans by the transfer of the glucosyl moiety from the sugar-nucleotide to the nonreducing end of the growing polyglucan chain [1,3,5].

Multiple SS isoforms have been described in plants: up to five SS isoforms have been categorized according to conserved sequence relationships (soluble forms SSI, SSII, SSIII, SSIV and SSV, and the granule-bound enzymes GBSSI and GBSSII) [1–3,6–10]. Each SS isoform has a specific role in determining the final structure of starch, i.e. GBSSs are involved in amylose synthesis, whereas the soluble forms have been postulated to participate in amylopectin synthesis, but also have a nonessential role in amylose production [1,3,7,8,11]. Indeed, it has been described that each SS soluble isoform has a different role in amylopectin biosynthesis: whilst SSII and SSIII have a major role in the synthesis of amylopectin, it has been suggested that SSI is mainly involved in the synthesis of small chains of this fraction. Furthermore, SSIV has been found recently to be involved in the control of the number of starch granules and starch granule initiation [6,8–10,12]. Indeed, it has been reported that different starch biosynthetic enzymes (including several SS isoforms) are capable of associating in a multisubunit complex, and that these interactions may be of physiological importance [13,14].

One of the soluble SS isoforms, SSIII, has been postulated to play a regulatory role in starch biosynthesis. Structural analysis of two insertional mutants at the *AtSS3* gene locus has revealed that SSIII deficiency causes a starch excess phenotype and an increase in total SS activity [8]. It has also been described that the N-terminal region of SSIII can interact with SSI [13]. The possible regulatory role of this protein makes this isoform a potential target for the manipulation of the level and quality of plant starch. However, little is known about the role of SSIII in starch synthesis and the structure–function relationship of this protein.

SSIII from higher plants contains two regions: (i) an N-terminal domain, which includes the transit peptide for plastid localization and a noncatalytic SSIII-specific domain; and (ii) a C-terminal domain, the catalytic domain (CD), common to all SS isoforms [15–17]. It has been described that the N-terminal region functions as a carbohydrate-binding module (CBM) [18,19]. Based on bioinformatic analyses, we have described that the N-terminal domain of *Arabidopsis thaliana* SSIII encodes three starch-binding domains (SBDs) named D1, D2 and D3 [20].

The SBDs have been described as noncatalytic modules, related to the CBM family. Sequence comparison established nine CBM families: (i) CBM20, i.e. the C-terminal SBD from *Aspergillus niger* glucoamylase; (ii) CBM21, located at the N-terminal domain in amylases; (iii) CBM25, containing one (i.e. β-amylase from *Bacillus circulans*) or two (i.e. *Bacillus* sp. α-amylase) modules; (iv) CBM26, mostly organized in tandem repeats (i.e. C-terminal domains from *Lactobacillus manihotivorans* α-amylase); (v) CBM34, present in the N-terminal domains of neopullulanase, maltogenic amylase and cyclomaltodextrinase; (vi) CBM41, N-terminal SBDs, present mostly in bacterial pullulanases; (vii) CBM45, originating from eukaryotic proteins from the plant kingdom (i.e. N-terminal modules of α-amylases and α-glucan water dikinases); (viii) CBM48, modules with glycogen-binding function (including SBD from the GH13 pullulanase and regulatory domains of mammalian AMP-activated protein kinase); and (ix) CBM53, SBD modules from SSIII [21–23] (http://www.cazy.org).

Recently, we have characterized the full-length SSIII enzyme from *A. thaliana*, as well as truncated isoforms lacking one, two or three SBDs, and also the recombinant SBDs. We propose that SBDs, in particular the D23 region, have a regulatory role in SSIII activity, showing starch-binding capacity and also modulating the catalytic properties of the enzyme [19]. To extend the information about the role of the noncatalytic SBD regions and their effect on the C-terminal CD, we further explored the amino acids of the N-terminal region responsible for SSIII regulation. We found evidence indicating that two regions, D(316–344) in the D2 domain and D(495–535) in the D3 domain, are involved in the interaction with CD, and that this interaction enhances the catalytic activity of the enzyme. Our results show that the interaction between SBDs and CD, as well as the full starch-binding capacity of the D2 domain, are necessary for the full catalytic activity of SSIII.

Results

Interaction between the N- and C-terminal domains of SSIII from *A. thaliana*

We propose that the N-terminal SBDs have a regulatory role, modulating the catalytic properties of the C-terminal domain of SSIII, which contains the catalytic site. Thus, we evaluated possible intramolecular interactions between the N-terminal SBDs and the C-terminal CD, and their effect on the regulatory properties of SSIII. To investigate this, we used the full N-terminal region of SSIII (D123 protein, containing the three SBDs, residues 22–575), CD (residues 576–1025) and different truncated and modified SBD proteins, as shown in Fig. 1.

First, we explored a potential protein–protein interaction between D123 and CD. We used two independent methods: (i) an *in vitro* pull-down assay using purified D123 protein and an extract expressing the recombinant CD protein; and (ii) a far western blotting assay in parallel with the pull-down technique to demonstrate the direct interaction of D123 with CD (Fig. 2). After incubation of the CD extract with the Ni^{2+} resin containing D123, two protein bands were observed after SDS-PAGE analysis (Fig. 2A, lane 1): a 64 kDa band, corresponding to D123, and a 48 kDa band, corresponding to the CD protein as detected by western blot analysis (Fig. 2A, bottom panel). The D123 protein bound to the Ni^{2+} resin incubated with an *Escherichia coli* extract not expressing CD (Fig. 2A, lane 2) and the Ni^{2+} resin with the extract alone (Fig. 2A, lane 3) did not show the presence of any protein band, indicating that the interaction is specific. Controls using pre-immune serum were consistently negative (not shown). Furthermore, the interaction between D123 and CD was confirmed by far western blotting experiments. Recombinant CD_{His} was purified, electrophoresed by SDS-PAGE and transferred to a poly(vinylidene difluoride) membrane (Fig. 2B, lanes 1–3). The membrane in lane 1 was incubated with an *E. coli* extract expressing the D123 protein, blocked and finally developed using an anti-D123 serum. A band corresponding to the D123 protein was detected (Fig. 2B, lane 1) with antibodies raised against *Agrobacterium tumefaciens* glycogen synthase

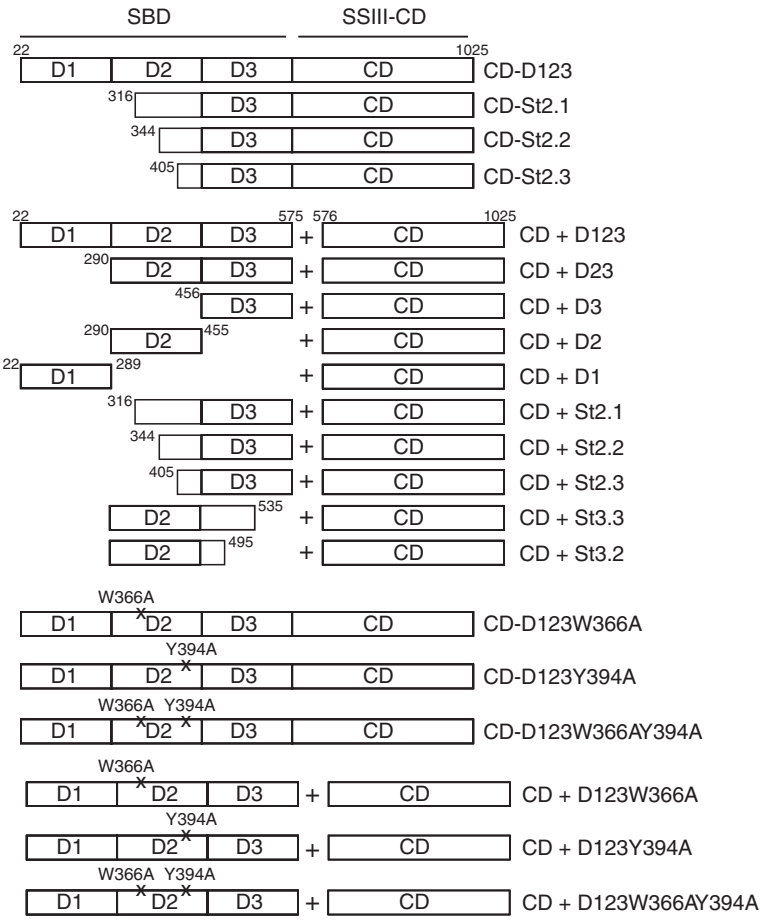

Fig. 1. Schematic representation of the peptides used in this study: CD–D123, full-length SSIII from *A. thaliana* lacking the transit peptide; SBD, starch-binding domain; CD, catalytic domain; D123, N-terminal domain containing the three SBDs; D23, truncated isoform lacking the D1 domain; CD–St2.1, CD–2.2 and CD–2.3, truncated proteins lacking different regions in the D2 domain; D1, D2, D3, individual SBD modules; St2.1, St2.2, St2.3, St3.3, St3.2, truncated proteins lacking different regions of the D2 or D3 domains; D123W366A, D123Y394A, modified D123 enzymes in which the aromatic residues have been replaced by alanine; D123W366Y394, double-mutated protein. The abbreviations for all co-expressed proteins are shown on the right-hand side of the figure. The locations of the different amino acids are indicated above each peptide.

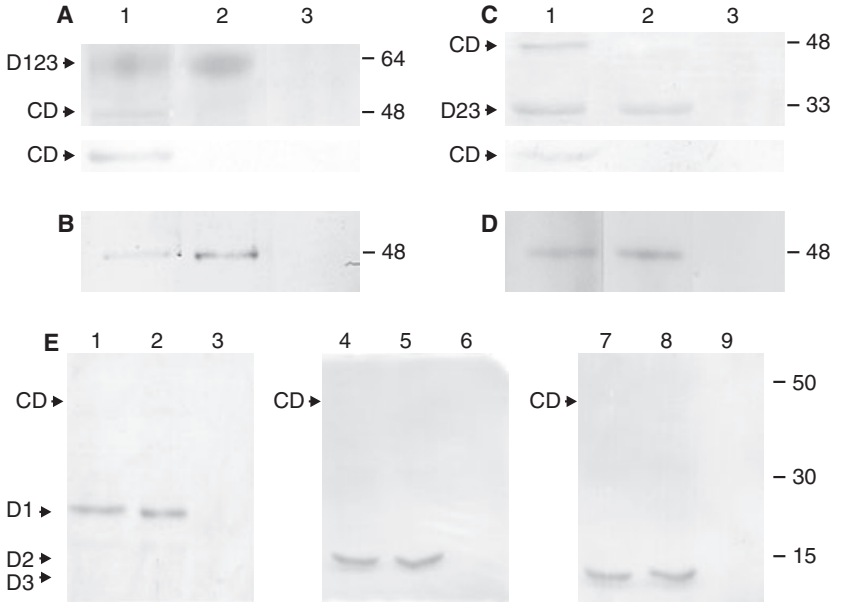

Fig. 2. (A) SDS-PAGE analysis of pull-down assays of recombinant D123 and CD proteins. Lane 1, CD protein was recovered together with D123; lane 2, recovered D123 bound to Ni^{2+} resin; lane 3, absence of CD rules out nonspecific binding to the resin (control). At the bottom of each lane, a western blot analysis illustrating the presence of CD is shown. (B) Analysis of CD and D123 interaction by far western blotting. Recombinant CD_{His} was subjected to SDS-PAGE and immunoblotting. The membrane in lane 1 was incubated with D123 and the protein was detected using anti-D123 serum. Other membranes containing electroblotted CD were revealed with anti-GS (lane 2) or anti-D123 (lane 3) serum. (C) Pull-down experiments of recombinant D23 and CD. The pull-down assay was performed as described for D123. Lane 1, D23 + CD; lane 2, D23; lane 3, CD. Western blot analysis of CD is shown below the figure. (D) Far western blot experiments of D23 and CD interaction. Lane 1, CD incubated with D23 and detected using anti-D123; CD was detected with anti-GS (lane 2) or anti-D123 (lane 3) serum. (E) Pull-down assays for D1 (left panel), D2 (middle panel) and D3 (right panel). The first lane of each panel (lanes 1, 4 and 7) corresponds to each SBD incubated with CD extract. Lanes 2, 5 and 7 correspond to D1, D2 and D3, respectively, without incubation with CD. Lanes 3, 6 and 9 correspond to D1, D2 and D3 eluted from Ni^{2+} resin.

(anti-GS serum, Fig. 2B, lane 2). The rf value for this band matches that expected for the CD_{His} protein. A control in which the CD protein was detected with anti-D123 serum was included to show the specificity of the antibodies used (Fig. 2B, lane 3). Thus, far western experiments confirmed the results obtained in the pull-down assays, showing that there is a physical interaction between the N- and C-terminal domains of SSIII *in vitro*.

Mapping of the CD-binding region in the N-terminal SBDs

In order to identify the SBD region required for the SBD–CD interaction, we performed pull-down assays using the N-terminal-truncated proteins D23, D1, D2 and D3. We determined a positive interaction between protein D23 and CD (Fig. 2C, lane 1), and this result was also confirmed by far western blotting (Fig. 2D). However, a lack of interaction was observed in pull-down experiments in which D1, D2 or D3 proteins bound to an Ni^{2+} resin were incubated in the presence of the cell extract containing recombinant CD (Fig. 2E). SDS-PAGE analysis did not reveal the presence of any protein band, indicating that the individual SBDs are unable to interact with CD under these experimental conditions.

To further investigate which region in the D23 protein contains the interaction domain, we performed pull-down assays using truncated proteins, named St2.1, St2.2, St2.3, St3.2 and St3.3 (see Fig. 1). We determined a positive interaction between St2.1 and St3.3 with CD (Fig. 3A, B), whereas St2.2, St2.3 and St3.2 proteins showed no interaction with CD (Fig. 3C). These results indicate that two long loop regions are required to interact with CD (Fig. 3D): they span residues 316–344 in the D2 domain [D(316–344)] and residues 495–535 in the D3 domain [D(495–535)].

Co-expression and purification of CD and SBD recombinant proteins

Protein–protein interaction assays showed the existence of two different loop regions in D2 [D(316–344)] and

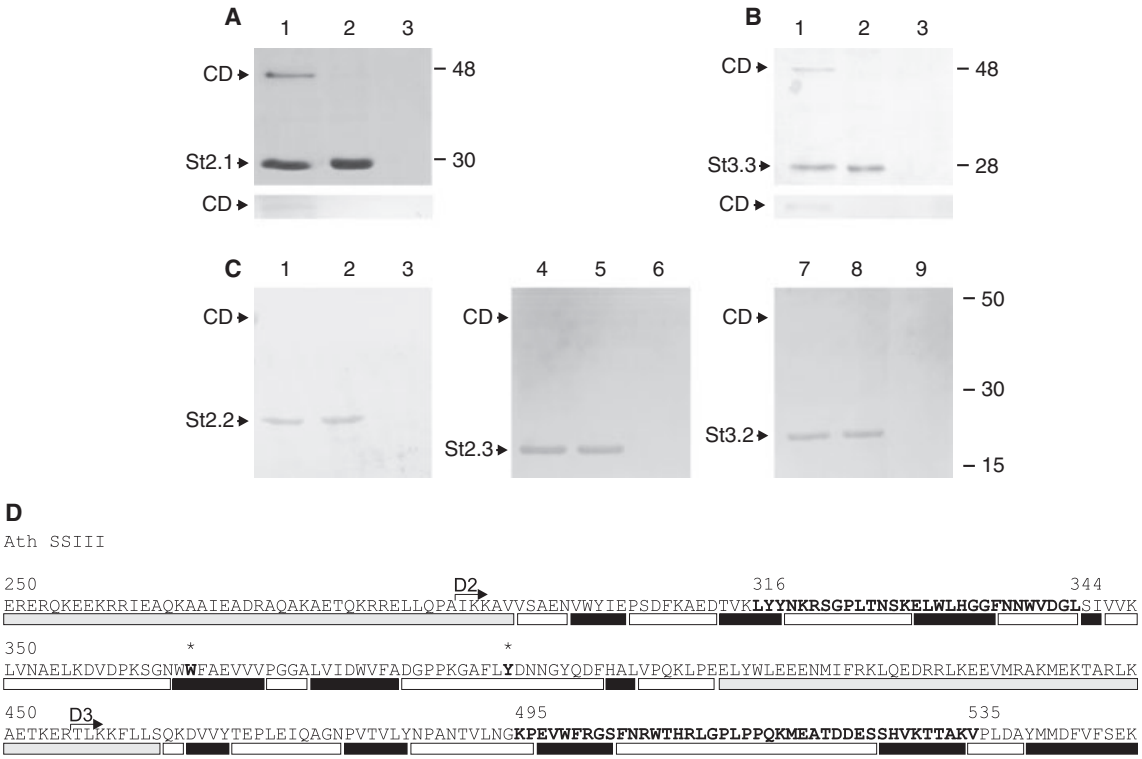

Fig. 3. SDS-PAGE analysis of pull-down assays of recombinant St2.1 (A) or St3.3 (B) and CD protein. The CD protein was recovered together with St2.1 (lane 1, A) or St3.3 (lane 1, B) protein. Lane 2, recovered St2.1 (A) or St3.3 (B) bound to Ni^{2+} resin. Lane 3 (A and B), absence of nonspecifically bound CD (control). At the bottom of each lane, a western blot analysis illustrating the presence of CD is shown. (C) Pull-down assays for St2.2 (left panel), St2.3 (middle panel) and St3.2 (right panel). The first lane of each panel (lanes 1, 4 and 7) corresponds to each St protein incubated with CD extract. Lanes 2, 5 and 8 correspond to St2.2, St2.3 and St3.2, respectively, without incubation with CD. Lanes 3, 6 and 9 correspond to St2.2, St2.3 and St3.2 recovery from Ni^{2+} resin. (D) Predicted secondary structure of *A. thaliana* SSIII (PSIPRED server [47]). Elements of secondary structure are highlighted by black bars (β strand), grey bars (helix) and white bars (coil). D2 and D3 domains are indicated by arrows. Stars indicate the positions of W366 and Y394. D(316–344) and D(495–535) regions are indicated in bold type.

D3 [D(495–535)], which are involved in the SBD–CD interaction *in vitro*. To evaluate the ability of SBDs and CD to interact in bacterial cells, we co-expressed the different His-tagged SBD proteins and untagged CD protein (cloned in the compatible pRSFDuet vector) in *E. coli* BL21-(DE3)-RIL cells. Purification was performed using an Ni^{2+} resin, as employed previously for the isolation of the individual recombinant proteins. SDS-PAGE and western blot analysis revealed the presence of D123 and CD, suggesting that their interaction can also occur *in vivo* (Fig. 4, lane D123). We also determined that D23, St2.1 and St3.3 proteins are able to interact with the CD fragment when co-purified from *E. coli* cells (Fig. 4, lanes D23, St2.1 and St3.3). Although the CD peptide was co-expressed successfully with D3, D2, D1, St2.2, St2.3 and St3.2 proteins, as revealed by denatured gel electrophoresis and western blot (not shown), we did not observe any co-purified protein band in SDS-PAGE analysis and western blot experiments (Fig. 4). These data are in agreement with the pull-down and far western assays, showing a lack of interaction for the individual SBDs and also in the absence of the D(316–344) and D(495–535) regions of the D2 and D3 domains, respectively.

Kinetic parameters of co-purified recombinant CD and different SBDs for the polysaccharide substrate

Kinetic parameters of co-expressed CD with D123 and truncated SBD proteins were determined. In the presence of a variable concentration of the polysaccharide, all the proteins displayed Michaelian kinetics. CD + D123 showed an $S_{0.5}$ value for glycogen of 0.32 ± 0.12 mg·mL^{-1} (Table 1), not significantly different from the $S_{0.5}$ value obtained for the full-length enzyme CD–D123 (0.28 ± 0.05 mg·mL^{-1}). CD + D123 displayed almost a six-fold decrease in $S_{0.5}$ for glycogen

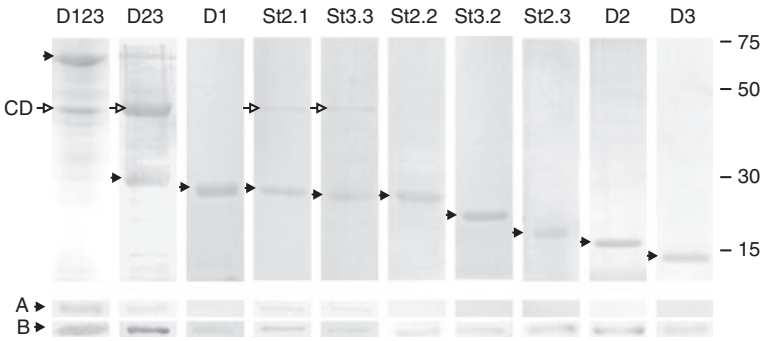

Fig. 4. SDS-PAGE analysis of co-expressed SBD proteins plus CD: D123, D23, D1, St2.1, St3.3, St2.2, St3.2, St2.3, D2 and D3. Black arrows indicate the different SBD proteins. White arrows indicate the presence of the CD protein. The presence of CD or SBD proteins was detected by western blot using anti-GS serum (A) or anti-D123 antibodies (B).

Table 1. Kinetic parameters of CD and CD + SBD proteins for glycogen.

Isoform	$S_{0.5}$ (mg·mL^{-1})	n_H	V_{max} (units·mg^{-1})
CD–D123	0.28 ± 0.05	1.0 ± 0.2	5.85 ± 0.37
CD	2.69 ± 0.16	1.2 ± 0.1	0.06 ± 0.02
CD+D123	0.32 ± 0.12	0.9 ± 0.3	0.58 ± 0.13
CD–D23	0.65 ± 0.15	1.1 ± 0.2	5.01 ± 0.48
CD–St2.1	0.59 ± 0.07	0.8 ± 0.2	4.73 ± 0.39
CD–St2.2	1.71 ± 0.21	1.2 ± 0.3	0.67 ± 0.05
CD–St2.3	1.76 ± 0.14	0.9 ± 0.1	0.61 ± 0.07
CD+D23	0.78 ± 0.13	1.0 ± 0.3	0.30 ± 0.07
CD+St2.1	1.05 ± 0.09	1.3 ± 0.2	0.41 ± 0.05
CD+St3.3	1.11 ± 0.10	1.1 ± 0.2	0.44 ± 0.02
CD–D3	1.87 ± 0.41	1.3 ± 0.2	0.72 ± 0.20

with respect to CD alone (2.69 ± 0.16 mg·mL^{-1}), indicating that the addition of D123 increases the apparent affinity of the CD protein for the polysaccharide. However, the CD + D123 protein only partially restored the V_{max} value of the full-length enzyme (about a 10-fold increase in the V_{max} value with respect to CD, but a nearly 10-fold lower V_{max} value with respect to the CD–D123 enzyme; Table 1).

Table 1 also lists the kinetic parameters of CD + D23 which lacks the D1 domain in the SBD peptide. This protein showed an $S_{0.5}$ value for glycogen of 0.78 ± 0.13 mg·mL^{-1} and a V_{max} value of 0.30 ± 0.07 U·mg^{-1}. Thus, CD + D23 completely restored the apparent affinity for glycogen with respect to the CD–D23 protein and, partially, its V_{max} value (Table 1). Indeed, we determined the kinetic parameters of CD + St2.1 and CD + St3.3. Both proteins showed a slight increase in the $S_{0.5}$ value for glycogen with respect to the CD + D23 protein; a partial restoration of the V_{max} value with respect to the CD–D23 protein was also observed (Table 1).

It is worth mentioning that we also determined the kinetic parameters of the SBD proteins and CD purified separately and mixed in a test-tube. We determined that, under saturating conditions of both substrates, the addition of 3 : 1, 2 : 1 and 1 : 1 molar amounts of the different SBD proteins plus CD in the test-tube produced similar kinetic parameters to those obtained from the co-purified enzymes. We also assayed the activity of the CD plus D3, D2, D1, St2.2, St2.3 and St3.2 proteins co-expressed or purified separately and mixed in a 1 : 1 molar ratio. In agreement with the results obtained in the protein interaction assays, we could not measure any glycosyltransferase activity in the co-purification experiments. Moreover, the individual proteins purified separately and mixed in the test-tube did not show any changes in their kinetic parameters when compared with the CD enzyme (not shown). The latter results agree with the lack of interaction between the individual SBD domains and CD, and also indicate that the presence of D3, D2, D1 or the truncated St2.2, St2.3 or St3.2 proteins alone plus CD does not affect the kinetic parameters for the polysaccharide substrate.

We also determined the kinetic parameters of the truncated CD–St2.1, CD–St2.2 and CD–St2.3 proteins (see Fig. 1). The CD–St2.1 protein showed no significant changes in the $S_{0.5}$ and V_{max} values relative to the CD–D23 enzyme. However, both the CD–St2.2 and CD–St2.3 proteins displayed a decrease in the apparent affinity for glycogen of about three-fold, and also an eight-fold decrease in V_{max} with respect to the CD–D23 enzyme (Table 1). Thus, the deletion of the $D_{316–344}$ region dramatically affects both the $S_{0.5}$ value for glycogen and the V_{max} value of the protein, showing similar kinetic parameters when compared with the CD–D3 enzyme (Table 1).

Kinetic parameters of co-purified recombinant CD and different SBDs for ADPGlc

Table 2 shows the kinetic parameters of the different SSIII enzymes for ADPGlc. In contrast with the total restoration of the $S_{0.5}$ values observed when using glycogen as a nonsaturating substrate, the CD + D123

Table 2. Kinetic parameters of CD and CD + SBD proteins for ADPGlc.

Isoform	$S_{0.5}$ (mM)	n_H	V_{max} (units·mg^{-1})
CD-D123	4.08 ± 0.49	1.1 ± 0.3	5.53 ± 0.52
CD	0.28 ± 0.05	1.0 ± 0.2	0.06 ± 0.01
CD+D123	0.95 ± 0.18	1.1 ± 0.2	0.60 ± 0.14
CD–D23	2.56 ± 0.54	2.0 ± 0.5	5.26 ± 0.48
CD–St2.1	2.39 ± 0.17	1.8 ± 0.2	4.95 ± 0.41
CD–St2.2	1.77 ± 0.15	1.1 ± 0.3	0.55 ± 0.05
CD–St2.3	1.68 ± 0.13	0.9 ± 0.1	0.49 ± 0.02
CD+D23	0.62 ± 0.14	1.8 ± 0.4	0.43 ± 0.10
CD+St2.1	0.59 ± 0.03	1.6 ± 0.3	0.48 ± 0.07
CD+St3.3	0.81 ± 0.09	1.1 ± 0.1	0.43 ± 0.03
CD–D3	1.74 ± 0.12	1.2 ± 0.2	0.57 ± 0.03

protein only partially restored the apparent affinity of the full-length enzyme for ADPGlc. Thus, the CD + D123 protein displayed an $S_{0.5}$ value about four-fold higher than CD and about 4.5-fold lower than the full-length enzyme (Table 2). Similar results were obtained with CD + D23, CD + St2.1 and CD + 3.3 proteins. These enzymes restored only partially the apparent affinity for ADPGlc and the catalytic efficiency with respect to the CD–D23 protein (Table 2). Similar to that observed in the kinetic assays for the polysaccharide substrate, the individual proteins purified separately, CD + D3, CD + D2, CD + D1, CD + St2.2, CD + St2.3 and CD + St3.2, did not show any changes in their kinetic parameters for the sugar nucleotide with respect to CD (not shown).

We also determined the kinetic parameters of the truncated proteins CD–St2.1, CD–St2.2 and CD–St2.3 for ADPGlc. A slight decrease in the $S_{0.5}$ value for ADPGlc was observed for the CD–St2.1 protein with respect to CD–D23. Indeed, no significant changes in V_{max} were observed between these proteins (Table 2). However, both CD–St2.2 and CD–St2.3 showed a decrease of about 30% in $S_{0.5}$ for ADPGlc, and also a decrease of nearly 10-fold in V_{max} with respect to CD–D23, displaying similar kinetic parameters to those obtained for the CD–D3 enzyme (Table 2).

Integrity of the D2 domain is necessary for full starch-binding activity

One of the best-characterized SBDs is glucoamylase-1 (GA-1) from *Aspergillus niger*, a member of the CBM20 family [24]. It has been established that different tryptophan residues are important for the binding activity and/or stability of this C-terminal SBD [25–27]. The SBD from GA-1 contains two independent polysaccharide-binding sites, which may be structurally and functionally different. It has been described that W590 is essential for binding activity in polysaccharide-binding site I and W563 is critical for site II, the latter having a tighter binding than site I [28]. Sequence alignment showed that W590 can be replaced by other aromatic residues (tyrosine in D1 and D2 and phenylalanine in D3), whereas W563 is conserved only in D2, but not in the D1 or D3 domains. Moreover, on the basis of bioinformatics analysis, we found a high structural similarity between GA-1 SBD and the D2 domain from SSIII [20]. Binding assays indicated that D2 has the highest starch-binding capacity (K_{ad} = 11.8 ± 1.5 mL·g^{-1}), whereas D1 and D3 do not have an important contribution to binding (K_{ad} = 0.6 ± 0.1 and 2.1 ± 0.3 mL·g^{-1}, respectively).

Thus, we decided to eliminate the putative polysaccharide-binding sites in the D2 domain of the full SBD region from SSIII (W366 and Y394, SSIII numbering). For this purpose, we generated the modified proteins D123W366A, D123Y394A and the double mutant D123W366AY394A.

We characterized the adsorption of the mutated proteins to raw starch at different protein concentrations, and also the effect of these mutations on SSIII kinetics. Figure 5 shows the adsorption isotherms for the binding of D123, D123W366A, D123Y394A and D123W366AY394A. D123 binds starch with high affinity (K_{ad} = 22.0 ± 0.8 mL·g^{-1}, [19]). D123W366A and D123Y394A proteins showed a three- and two-fold decrease in their affinity to starch (K_{ad} = 7.9 ± 1.0 and 11.2 ± 0.9 mL·g^{-1}, respectively), whereas D123W366AY394A showed a significant decrease (almost six-fold) in its binding affinity (K_{ad} = 3.8 ± 0.6 mL·g^{-1}).

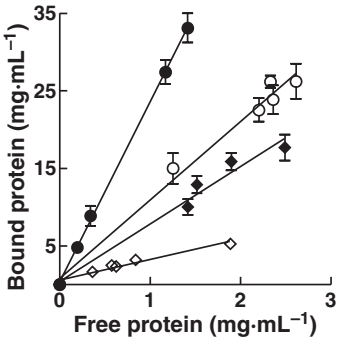

Fig. 5. Adsorption of purified SBD proteins to cornstarch: D123 (filled circles), D123W366A (filled diamonds), D123Y394A (open circles) and D123W366AY394A (open diamonds). Linear adsorption isotherms indicate the apparent equilibrium distribution of SBD proteins between the solid (bound protein, in milligrams per gram of starch) and liquid (free protein, in mg·mL^{-1}) phases at various protein concentrations. K_{ad} values (milliliters per gram of starch) represent the slope of each isotherm.

Effect of W366A and Y394A mutations on SSIII kinetics

We also determined the effect of mutations in the putative starch-binding sites I and/or II, and whether they affected SSIII kinetics. First, we confirmed, using pull-down assays, that the mutations in the starch-binding residues did not affect the interaction with CD (not shown). The $S_{0.5}$ value for the acceptor polysaccharides of the CD + D123W366A protein was about five-fold higher than that of the CD + D123 or full-length CD–D123 protein. In contrast, no significant changes were observed in the $S_{0.5}$ value for glycogen when using CD + D123Y394A (0.32 ± 0.13 mM) or the nonmutated protein (Table 3). In addition, both CD + D123W366A and CD + D123Y394A proteins showed similar V_{max} values when compared with the CD + D123 protein. Thus, both modified proteins partially restored the V_{max} values for the CD–D123 enzyme, but displayed about a 12-fold increase in V_{max} with respect to CD alone. Finally, the CD + D123 W366AY394A protein showed an $S_{0.5}$ value for glycogen similar to that of CD (about 10-fold higher than the $S_{0.5}$ value for the nonmodified enzyme), an n_H value of 1.8 ± 0.4 and a slight decrease in V_{max} with respect to the CD + D123 protein (Table 3).

However, no significant changes were observed in the $S_{0.5}$ values for ADPGlc, compared with the CD + D123 enzyme, when the mutated SBD proteins CD + D123W366A, CD + D123Y394A and CD + D123W366AY394A were assayed. Nevertheless, an increase in n_H values was observed (Table 4). Moreover, we observed only slight changes in V_{max} values for these enzymes with respect to the CD + D123 protein, suggesting that the mutations did not affect the kinetics for ADPGlc (Table 4).

We also evaluated the kinetic parameters for the full-length mutated proteins CD–D123W366A, CD–D123Y394A and CD–D123W366AY394A. None of the mutations greatly affected V_{max} or n_H relative to the values for the CD–D123 enzyme. Moreover, CD–D123W366A and CD–D123W366AY394 showed an increase in $S_{0.5}$ value for glycogen of about five- and 10-fold, respectively, compared with the CD–123 enzyme (Table 3). However, only about a 20% decrease in $S_{0.5}$ for ADPGlc was observed for the full-length mutated proteins (Table 4), in agreement with the results obtained from co-expression experiments.

Table 3. Kinetic parameters of mutated proteins for glycogen.

Isoform	$S_{0.5}$ (mg·mL^{-1})	n_H	V_{max} (units·mg^{-1})
CD+D123W366A	1.73 ± 0.10	1.0 ± 0.2	0.77 ± 0.11
CD+D123Y394A	0.32 ± 0.13	1.2 ± 0.3	0.64 ± 0.13
CD+D123W366AY394A	3.0 ± 0.29	1.8 ± 0.4	0.36 ± 0.09
CD–D123W366A	1.55 ± 0.11	0.8 ± 0.1	4.58 ± 0.35
CD–D123Y394A	0.26 ± 0.03	1.0 ± 0.2	4.43 ± 0.41
CD–D123W366AY394A	2.99 ± 0.23	1.1 ± 0.3	4.50 ± 0.47

Table 4. Kinetic parameters of mutated proteins for ADPGlc.

Isoform	$S_{0.5}$ (mM)	n_H	V_{max} (units·mg^{-1})
CD+D123W366A	0.91 ± 0.14	2.1 ± 0.4	0.86 ± 0.22
CD+D123Y394A	0.76 ± 0.10	3.3 ± 0.3	0.96 ± 0.26
CD+D123W366AY394A	0.69 ± 0.14	1.9 ± 0.3	0.36 ± 0.11
CD–D123W366A	3.12 ± 0.29	1.1 ± 0.1	4.37 ± 0.03
CD–D123Y394A	3.01 ± 0.31	0.9 ± 0.1	4.50 ± 0.04
CD–D123W366AY394A	3.35 ± 0.25	1.2 ± 0.2	4.42 ± 0.03

Discussion

In the last decade, there has been an increasing demand for starch in many industrial processes, such as food, pharmaceutical and bioethanol production. Thus, a better understanding of starch biosynthesis, in particular the structure–function relationship and regulatory properties of the enzymes involved in its production, may provide a powerful tool for the planning of new strategies to increase plant biomass, as well as to improve the quality and quantity of this polymer [29,30]. However, the structure, function and regulation of SSIII have been less well studied [15,17–20]. Several reports have proposed that this enzyme plays a key regulatory role in the synthesis of starch in *Arabidopsis* [8,31,32], and it has been found to be involved in starch granule initiation [12].

Recently, we have described that the SSIII isoform from *A. thaliana* encodes three SBDs in its N-terminal region [19,20]. SBDs are noncatalytic modules related to the CBM family, and, in particular, the SBDs from SSIII have been grouped into the CBM53 family [21]. Analysis of the full-length and truncated SSIII isoforms lacking one, two or three SBDs revealed that these N-terminal modules are important in starch binding, and also in the regulation of SSIII catalytic activity [19]. In order to investigate possible protein–protein interactions and their effect on enzyme kinetics, we performed pull-down, far western blotting and co-expression experiments between the N- and C-terminal domains of SSIII. *In vitro* assays revealed an interaction between the D123 domain and CD. Furthermore, when co-expressed in *E. coli* cells, the two proteins co-purified, in agreement with

in vitro studies. Removal of the D1 region did not prevent the positive interaction between D23 and CD, indicating that the D1 region does not have a significant contribution to the binding process. Analysis of the interaction between truncated D23 proteins and CD revealed the importance of two different loop regions which are essential for the interaction: D(316–344) in the D2 domain and D(495–535) in the D3 domain. This result is in agreement with our previous studies using truncated SSIII isoforms, showing the importance of the D23 domain in starch binding and the modulation of SSIII activity [19]. A similar conclusion has been reached for other enzymes involved in starch (or bacterial glycogen) biosynthesis, such as ADPGlc PPases. It has been described that this enzyme is composed of two domains with a strong interaction between them, and that this interaction is important in the regulation of both its activity and allosteric properties [33,34].

Recent studies have shown that different starch biosynthetic enzymes, such as SSIIa, SSIII and branching enzymes SBEIIa and SBEIIb from maize, associate into a multisubunit high molecular weight complex [13,35]. *Zea mays* SSIII presents two well-differentiated structural domains in the N-terminal region: an N-terminal-specific region (residues 1–726) and an SSIIIHD region (containing the three SBDs, residues 727–1216), distinct from the catalytic domain formed by the C-terminal portion of the protein [13,32]. Whereas the ZmSSIIIHD portion binds to SSI, residues 1–726 (involved in branching enzyme binding) are not present in *A. thaliana* SSIII. Computational predictions identified coiled-coil domains in the SSIIIHD region that could explain both protein recognition and glucan binding [35]. Thus, it has been proposed that SSIIIHD may have different roles in protein–protein interaction and polysaccharide binding.

Analysis of the starch-binding capacity of the individual SBDs has indicated that D2 has the highest binding affinity relative to D1 or D3. It is important to note that previous bioinformatics analysis has revealed that the D2 domain has a high structural similarity to the SBD of GA-1 from *Aspergillus niger* [20]. It has been described that the GA-1 SBD has two starch-binding sites (both involving tryptophan residues) which are essential for the induction of conformational changes in the starch structure [25–27]. Moreover, the alignment of the amino acid sequences of SBDs from CBM20s (including some mammalian proteins, such as laforin, involved in the regulation of glycogen metabolism), CBM21s, CBM48s and CBM53s has revealed only subtle differences in the polysaccharide-binding sites, showing a high degree of conservation of the tryptophan in binding site II and an aromatic residue (mainly tryptophan or tyrosine) in binding site I [22]. We have shown that the tryptophan residue involved in binding site II is conserved in the D2 protein (W366); however, a tyrosine residue (Y394) is present in binding site I. Structural analysis has revealed that both aromatic residues are well conserved in the three-dimensional structure [20], suggesting that the W366 and Y394 residues of the D2 domain may play a role similar to that of binding sites I and II of GA-1. Mutations of W366 and Y394 in D123 decreased the starch-binding capacity by three- and two-fold, respectively, whereas the double mutant D123W366AY394A showed a six-fold reduction in affinity, indicating that both residues are important in the binding of the polysaccharide.

It has been reported that the SBD modules present in microbial starch-degrading enzymes promote the attachment to the polysaccharide, increasing its concentration at the active site of the enzyme, which leads to an increase in the starch degradation rate [36]. It is important to note that the aromatic residues W366 and Y394 involved in starch binding are located in the D2 domain, between the D(316–344) and D(495–535) interacting loops (see Fig. 3D). Indeed, it has also been suggested that the tandem arrangement of SBDs in lactobacilli could be suited to the disruption of the starch structure, analogous to the two binding sites of *Aspergillus niger* GA-1, and this arrangement may be important to improve starch binding [37,38].

In addition, the α-amylase from some *Lactobacillus* species contains in-tandem SBDs linked by intermediary regions rich in serine or threonine [36,39], as well as the *Rhizopus oryzae* glucoamylase [40]. These linker sequences may increase the random coil regions and mobility of SBDs. However, α-amylases containing SBDs lacking the flexible region are catalytically more efficient in degrading the polysaccharide substrates. Surprisingly, SBD linkers from *A. thaliana* show low percentages of threonine and serine residues (2% for D1–D2 and 6% for D2–D3 linkers), suggesting a certain rigidity of the N-terminal D123 domain, and thus a higher efficiency in starch binding.

Kinetic analysis of co-purified CD with D123, D23, St2.1 or St3.3 proteins showed that the addition of these SBD proteins increased the apparent affinity of SSIII for glycogen. Moreover, kinetic experiments are in agreement with the protein–protein interaction assays, suggesting the importance of the interaction among D(316–344), D(495–535) and CD in the modulation of SSIII activity. In contrast, the individual SBD proteins D1, D2, D3 or St2.2, St2.3 and St3.2 did not show any effect on catalysis. When analyzing

the functional consequences of aromatic amino acid substitution on starch binding and SSIII kinetics, we found that the CD + D123W366A protein showed a strong reduction in the polysaccharide apparent affinity (four- to six-fold), whereas the CD + D123Y394 protein did not show significant changes in the $S_{0.5}$ value for glycogen. However, the double-mutated protein CD + D123W366Y394 showed similar $S_{0.5}$ values to CD for the polysaccharide. Similar results were obtained with the full-length mutated enzymes; however, an almost complete restoration of the V_{max} value was observed for these proteins, suggesting an important role of the CD–SBD linker region.

However, no significant changes in the kinetic parameters for ADPGlc were observed in the mutated proteins relative to CD + D123. These results indicate that, although both aromatic residues are important in starch binding, W366 makes the greatest contribution in the regulation of SSIII activity by modulating the affinity of the acceptor polysaccharide. As mentioned above, it has been reported that enzyme adsorption to the polysaccharide is a prerequisite for raw starch hydrolysis by bacterial amylases [39,41]. Our results are in agreement with these findings, suggesting that efficient binding of starch in the D2 domain is important to modulate SSIII activity.

Our data showed a complete restoration of the apparent affinity for the polysaccharide in the presence of different co-purified SBDs, but a partial restoration of the $S_{0.5}$ and V_{max} values for ADPGlc. Characterization of CD–23, CD–St2.1 and CD–St2.2 proteins also showed similar $S_{0.5}$ values for glycogen relative to the respective co-purified proteins. However, an almost complete restoration of the $S_{0.5}$ and V_{max} values for ADPGlc was observed for CD–23 and CD–St2.1, but not for the CD–St2.2 protein, showing the importance of the interacting region in the D2 domain and the linker region connecting CD and SBDs for full SSIII activity. In accordance with our results, it is possible to postulate that a rigid interaction between the N-terminal SBD region and the CD protein is essential for full recovery of SSIII catalytic activity.

In conclusion, our findings support the importance of the loop regions D(316–344) and D(495–535) for the interaction between the N-terminal SBDs and CD. Our data also show that the full integrity of the starch-binding capacity, particularly of the D2 domain, modulates the activity of SSIII. Although it is not currently clear whether there is a common biochemical mechanism underlying SBD participation, it is possible to postulate that the protein–protein interaction between the D(316–344) and D(495–535) regions and CD plays an important role in the promotion of starch binding to CD, subsequently increasing its concentration in the active site, and thus determining the catalytic efficiency of the protein for the polysaccharide. Although the complete mechanism of SSIII activity modulation by SBD cannot be deduced until the enzyme conformation is elucidated, the data presented here contribute to a better understanding of how SBDs modulate enzyme activity, as well as their importance and function in starch synthesis in plant cells.

Experimental procedures

Strain, culture media and expression vectors

Escherichia coli XL1Blue and BL21-(DE3)-RIL strains were used as hosts for this study. *Escherichia coli* strains were grown at 37 °C in Luria–Bertani medium [19]. Expression vectors derived from pET32c contained a C-terminal His-tag. The different constructs are shown in Fig. 1. For the co-expression experiments, CD was cloned as expressed without any tags (see below).

Construction of the pNAL1 vector for the expression of CD of SSIII from *A. thaliana* and truncated proteins

The plasmid named pVAL3 containing the catalytic C-terminal domain of SSIII (1374 bp) was used as template for cDNA synthesis [19]. cDNA corresponding to CD was PCR amplified using *Pfu* polymerase (Promega, Madison, WI, USA) and the following primers: CDfw, AGAGC ATATGCACATTGTTCAT; CDrv, AAACTCGAGTCAC TTGCGTGCAGAGTGATAGAGC. The resulting PCR product was digested with *Nde*I and *Xho*I and cloned into the pRSFDuet vector (Novagen, Madison, WI, USA). The new vector named pNAL1 encodes CD without any fusion tags. BL21-(DE3)-RIL *E. coli* competent cells were transformed with pNAL1 and used for expression analysis.

Truncated proteins were generated using the following primers: 2.1up, AAACATATGCTATATTACAATAAAA GG; 2.2up, AAACATATGTTATCTATCGTTGTAAAGC; 2.3up, AAACATATGCTTGTTCCTCAAAAACTTCC; 3.3rv, AAACTCGAGGACCTTAGCCGTAGTCTTCAC; 3.2rv, AAACTCGAGTTTTCCATTCAAAACCGTG.

Construction of site directed mutants

The mutated proteins D123W366A, D123Y394A and the double-modified protein D123W366AY394A were obtained using the QuickChange II site-directed mutagenesis kit (Stratagene, La Jolla, CA, USA). The pVAL19 vector which codifies for the D123 protein was used as the template for PCR amplification. The following primers (and their complements) were used (base substitutions in italic):

123W366A, CCAAAGAGCGGAAATTGG*GCG*TTCGCT GAAGTTG; 123Y394A, CTAAAGGAGCGTTTCTG *GCT*GACAATAATGGTTAC. The mutated sequences were confirmed by DNA sequencing.

Expression and purification of CD, CD_{His} SBDs, co-expressed and mutated recombinant proteins

Individual recombinant proteins were expressed and purified using a HiTrap chelating HP column (GE Healthcare Bio-Sciences, Upsalla, Sweden), as described previously [19]. For co-expression analysis, the bacterial cells were co-transformed with pNAL1 (encoding untagged CD) plus pVAL19, pVAL20, pVAL21, pVAL25, pVAL29 and pVAL31–pVAL38 (corresponding to D123, D23, D3, D2, D1, D123W366A, D123Y394A, D123W366AY394A, St2.1, St2.2, St2.3, St3.3 and St3.2 His_6-tag-containing proteins cloned in the pET32 vector). The co-expressed proteins were purified by Ni^{2+} chelating chromatography using the same protocol [19]. Active fractions were concentrated to $> 1\ mg{\cdot}mL^{-1}$, desalted and immediately used to determine the enzymatic activity. The presence of the different recombinant proteins was monitored in chromatographic fractions by measuring the SS activity, SDS-PAGE and immunoblotting.

Detection of protein–protein interactions by pull-down assays and far western blotting

Pull-down assays were carried out as follows: purified His_6-tagged SBD proteins were bound to an Ni^{2+} -Sepharose high-performance resin (GE Healthcare Bio-Sciences) previously equilibrated with binding buffer (20 mM NaH_2PO_4, pH 7.4, 50 mM NaCl, 1 mM 2-mercaptoethanol and 20 mM imidazole), followed by incubation with 1 mg of cell extract from *E. coli* BL21-(DE3)-RIL transformed with pNAL1 plasmid and rotation for 1 h at 30 °C. After washing three times with binding buffer, the resin was centrifuged for 3 min at 500 ***g*** and the supernatant was discarded. The bound proteins were eluted from the resin by the addition of 300 mM imidazole, and subjected to SDS-PAGE analysis and immunoblotting.

Far western blotting was performed as described previously [42] with minor modifications. First, recombinant CD_{His} was separated by SDS-PAGE and transferred onto a poly(vinylidene difluoride) membrane. The membrane was then blocked in $NaCl/P_i$ buffer containing 3% BSA and 0.1% (v/v) Tween-20, and incubated overnight at 4 °C with $2\ \mu g{\cdot}mL^{-1}$ of the bait proteins. After this, the membrane was washed three times for 10 min with $NaCl/P_i$ buffer containing 0.1% Tween-20. SBD proteins bound to CD_{His} were detected by incubation with antibodies raised against recombinant D123 protein (anti-D123). Controls were incubated with anti-GS serum. The antigen–antibody complex was visualized with alkaline phosphatase-conjugated a-mouse IgG or a-rabbit IgG, followed by staining with 5-bromo-4-chloroindol-2-yl phosphate and nitroblue tetrazolium [43].

Additional methods

Binding assays were performed by the adsorption of different SBD recombinant proteins to raw starch, and the adsorption constant (K_{ad}, in milliliters per gram of starch) was determined from the slope, as reported previously. All the determinations were performed at least in triplicate and the average values ± SD are reported [19,39]. SS activity was determined using a radiochemical method [44]. All kinetic parameters are the means of at least three determinations and are reproducible within ± 10%. SDS-PAGE was performed using 12% gels as described by Laemmli [45]. Gels were developed by Coomassie blue staining or electroblotted onto nitrocellulose (Bio-Rad, Hercules, CA, USA) or poly(vinylidene difluoride) (GE Healthcare Bio-Sciences) membranes. Electroblotted membranes were incubated with penta-His antibody (Qiagen, Valencia, CA, USA) or polyclonal antibodies raised against recombinant *Agrobacterium tumefaciens* glycogen synthase (anti-GS) [17] or anti-D123. The antigen–antibody complex was visualized as described above [43]. Total protein was determined as described by Bradford [46].

Acknowledgements

This work is dedicated to the memory of Professor Dr Rodolfo Ugalde who passed away in August 2009. We had the good fortune to know Rodolfo and interact with him in planning and discussing scientific experiments and other topics related to biochemistry. We wish to dedicate this work to him as a sign of immense regard for our former adviser, colleague and friend.

We are grateful to Jose Luis Burgos [Comision de Investigaciones Cientificas (CIC)] for excellent technical assistance and Dr María Corvi for helpful discussions and critical reading of the manuscript. This work was supported in part by grants from the Biotechnology Program of Universidad Nacional de General San Martin (UNSAM) (PROG07F/2-2007) and Consejo de Investigaciones Cientificas y Tecnicas (CONICET) (PIP 00237). NZW and HAV are doctoral fellows from CONICET. MVB and DGC are research members from CONICET.

References

1 Smith AM (2001) The biosynthesis of starch granules. *Biomacromolecules* **2**, 335–341.
2 Preiss J & Sivak MN (1998) Biochemistry, molecular biology and regulation of starch synthesis. *Genet Eng (NY)* **20**, 177–223.

3 Ball SG & Morell MK (2003) From bacterial glycogen to starch: understanding the biogenesis of the plant starch granule. *Annu Rev Plant Biol* **54**, 207–233.
4 Martin C & Smith AM (1995) Starch biosynthesis. *Plant Cell* **7**, 971–985.
5 Tetlow IJ, Morell MK & Emes MJ (2004) Recent developments in understanding the regulation of starch metabolism in higher plants. *J Exp Bot* **55**, 2131–2145.
6 Delvalle D, Dumez S, Wattebled F, Roldan I, Planchot V, Berbezy P, Colonna P, Vyas D, Chatterjee M, Ball S *et al*. (2005) Soluble starch synthase I: a major determinant for the synthesis of amylopectin in *Arabidopsis thaliana* leaves. *Plant J* **43**, 398–412.
7 Maddelein ML, Libessart N, Bellanger F, Delrue B, D'Hulst C, Van den Koornhuyse N, Fontaine T, Wieruszeski JM, Decq A & Ball S (1994) Toward an understanding of the biogenesis of the starch granule. Determination of granule-bound and soluble starch synthase functions in amylopectin synthesis. *J Biol Chem* **269**, 25150–25157.
8 Zhang X, Myers AM & James MG (2005) Mutations affecting starch synthase III in Arabidopsis alter leaf starch structure and increase the rate of starch synthesis. *Plant Physiol* **138**, 663–674.
9 Delrue B, Fontaine T, Routier F, Decq A, Wieruszeski JM, Van Den Koornhuyse N, Maddelein ML, Fournet B & Ball S (1992) Waxy *Chlamydomonas reinhardtii*: monocellular algal mutants defective in amylose biosynthesis and granule-bound starch synthase activity accumulate a structurally modified amylopectin. *J Bacteriol* **174**, 3612–3620.
10 Roldan I, Wattebled F, Mercedes Lucas M, Delvalle D, Planchot V, Jimenez S, Perez R, Ball S, D'Hulst C & Merida A (2007) The phenotype of soluble starch synthase IV defective mutants of *Arabidopsis thaliana* suggests a novel function of elongation enzymes in the control of starch granule formation. *Plant J* **49**, 492–504.
11 Ball S, Guan HP, James M, Myers A, Keeling P, Mouille G, Buleon A, Colonna P & Preiss J (1996) From glycogen to amylopectin: a model for the biogenesis of the plant starch granule. *Cell* **86**, 349–352.
12 Szydlowski N, Ragel P, Raynaud S, Lucas MM, Roldan I, Montero M, Munoz FJ, Ovecka M, Bahaji A, Planchot V *et al*. (2009) Starch granule initiation in Arabidopsis requires the presence of either class IV or class III starch synthases. *Plant Cell* **21**, 2443–2457.
13 Hennen-Bierwagen TA, Liu F, Marsh RS, Kim S, Gan Q, Tetlow IJ, Emes MJ, James MG & Myers AM (2008) Starch biosynthetic enzymes from developing maize endosperm associate in multisubunit complexes. *Plant Physiol* **146**, 1892–1908.
14 Tetlow IJ, Beisel KG, Cameron S, Makhmoudova A, Liu F, Bresolin NS, Wait R, Morell MK & Emes MJ (2008) Analysis of protein complexes in wheat amyloplasts reveals functional interactions among starch biosynthetic enzymes. *Plant Physiol* **146**, 1878–1891.
15 Li Z, Mouille G, Kosar-Hashemi B, Rahman S, Clarke B, Gale KR, Appels R & Morell MK (2000) The structure and expression of the wheat starch synthase III gene. Motifs in the expressed gene define the lineage of the starch synthase III gene family. *Plant Physiol* **123**, 613–624.
16 Dian W, Jiang H & Wu P (2005) Evolution and expression analysis of starch synthase III and IV in rice. *J Exp Bot* **56**, 623–632.
17 Busi MV, Palopoli N, Valdez HA, Fornasari MS, Wayllace NZ, Gomez-Casati DF, Parisi G & Ugalde RA (2008) Functional and structural characterization of the catalytic domain of the starch synthase III from *Arabidopsis thaliana*. *Proteins* **70**, 31–40.
18 Senoura T, Asao A, Takashima Y, Isono N, Hamada S, Ito H & Matsui H (2007) Enzymatic characterization of starch synthase III from kidney bean (*Phaseolus vulgaris* L.). *FEBS J* **274**, 4550–4560.
19 Valdez HA, Busi MV, Wayllace NZ, Parisi G, Ugalde RA & Gomez-Casati DF (2008) Role of the N-terminal starch-binding domains in the kinetic properties of starch synthase III from *Arabidopsis thaliana*. *Biochemistry* **47**, 3026–3032.
20 Palopoli N, Busi MV, Fornasari MS, Gomez-Casati D, Ugalde R & Parisi G (2006) Starch-synthase III family encodes a tandem of three starch-binding domains. *Proteins* **65**, 27–31.
21 Cantarel BL, Coutinho PM, Rancurel C, Bernard T, Lombard V & Henrissat B (2009) The Carbohydrate-Active EnZymes database (CAZy): an expert resource for glycogenomics. *Nucleic Acids Res* **37**, D233–D238.
22 Christiansen C, Abou Hachem M, Janecek S, Viksø-Nielsen A, Blennow A & Svensson B (2009) The carbohydrate-binding module family 20 – diversity, structure, and function. *FEBS J* **276**, 5006–5029.
23 Machovic M & Janecek S (2006) Starch-binding domains in the post-genome era. *Cell Mol Life Sci* **63**, 2710–2724.
24 Machovic M & Janecek S (2006) The evolution of putative starch-binding domains. *FEBS Lett* **580**, 6349–6356.
25 Giardina T, Gunning AP, Juge N, Faulds CB, Furniss CS, Svensson B, Morris VJ & Williamson G (2001) Both binding sites of the starch-binding domain of *Aspergillus niger* glucoamylase are essential for inducing a conformational change in amylose. *J Mol Biol* **313**, 1149–1159.
26 Penninga D, van der Veen BA, Knegtel RM, van Hijum SA, Rozeboom HJ, Kalk KH, Dijkstra BW & Dijkhuizen L (1996) The raw starch binding domain of cyclodextrin glycosyltransferase from *Bacillus circulans* strain 251. *J Biol Chem* **271**, 32777–32784.
27 Williamson MP, Le Gal-Coeffet MF, Sorimachi K, Furniss CS, Archer DB & Williamson G (1997)

Function of conserved tryptophans in the *Aspergillus niger* glucoamylase 1 starch binding domain. *Biochemistry* **36**, 7535–7539.
28 Sorimachi K, Le Gal-Coeffet MF, Williamson G, Archer DB & Williamson MP (1997) Solution structure of the granular starch binding domain of *Aspergillus niger* glucoamylase bound to beta-cyclodextrin. *Structure* **5**, 647–661.
29 Smith AM (2008) Prospects for increasing starch and sucrose yields for bioethanol production. *Plant J* **54**, 546–558.
30 Jobling S (2004) Improving starch for food and industrial applications. *Curr Opin Plant Biol* **7**, 210–218.
31 Edwards A, Fulton DC, Hylton C, Jobling SA, Gidley M, Rössner U, Martin C & Smith A (1999) A combined reduction in activity of starch synthases II and III of potato has novel effects on the starch of tubers. *Plant J* **17**, 251–261.
32 Gao M, Wanat J, Stinard PS, James MG & Myers AM (1998) Characterization of dull1, a maize gene coding for a novel starch synthase. *Plant Cell* **10**, 399–412.
33 Ballicora MA, Iglesias AA & Preiss J (2004) ADP-glucose pyrophosphorylase: a regulatory enzyme for plant starch synthesis. *Photosynth Res* **79**, 1–24.
34 Bejar CM, Ballicora MA, Gomez-Casati DF, Iglesias AA & Preiss J (2004) The ADP-glucose pyrophosphorylase from *Escherichia coli* comprises two tightly bound distinct domains. *FEBS Lett* **573**, 99–104.
35 Hennen-Bierwagen TA, Lin Q, Grimaud F, Planchot V, Keeling PL, James MG & Myers AM (2009) Proteins from multiple metabolic pathways associate with starch biosynthetic enzymes in high molecular weight complexes: a model for regulation of carbon allocation in maize amyloplasts. *Plant Physiol* **149**, 1541–1559.
36 Rodriguez-Sanoja R, Oviedo N & Sanchez S (2005) Microbial starch-binding domain. *Curr Opin Microbiol* **8**, 260–267.
37 Rodríguez-Sanoja R, Oviedo N, Escalante L, Ruiz B & Sánchez S (2009) A single residue mutation abolishes attachment of the CBM26 starch-binding domain from *Lactobacillus amylovorus* alpha-amylase. *J Ind Microbiol Biotechnol* **36**, 341–346.
38 Southall SM, Simpson PJ, Gilbert HJ, Williamson G & Williamson MP (1999) The starch-binding domain from glucoamylase disrupts the structure of starch. *FEBS Lett* **447**, 58–60.
39 Rodriguez-Sanoja R, Ruiz B, Guyot JP & Sanchez S (2005) Starch-binding domain affects catalysis in two *Lactobacillus* alpha-amylases. *Appl Environ Microbiol* **71**, 297–302.
40 Lin S-C, Liu W-T, Liu S-H, Chou W-I, Hsiung B-K, Lin I-P, Sheu C-C & Chang MD-T (2007) Role of the linker region in the expression of *Rhizopus oryzae* glucoamylase. *BMC Biochem* **8**, 9.
41 Leloup VM, Colonna P & Ring SG (1991) alpha-Amylase adsorption on starch crystallites. *Biotechnol Bioeng* **38**, 127–134.
42 Wu Y, Li Q & Chen XZ (2007) Detecting protein–protein interactions by far western blotting. *Nat Protoc* **2**, 3278–3284.
43 Bollag DM, Rozycki MD & Edelstein SJ (1996) *Protein Methods*, 2nd edn. Wiley-Liss, New York.
44 Ugalde JE, Parodi AJ & Ugalde RA (2003) De novo synthesis of bacterial glycogen: *Agrobacterium tumefaciens* glycogen synthase is involved in glucan initiation and elongation. *Proc Natl Acad Sci USA* **100**, 10659–10663.
45 Laemmli UK (1970) Cleavage of structural proteins during the assembly of the head of bacteriophage T4. *Nature* **227**, 680–685.
46 Bradford MM (1976) A rapid and sensitive method for the quantitation of microgram quantities of protein utilizing the principle of protein–dye binding. *Anal Biochem* **72**, 248–254.
47 Bryson K, McGuffin LJ, Marsden RL, Ward JJ, Sodhi JS & Jones DT (2005) Protein structure prediction servers at University College London. *Nucleic Acids Res* **33**, W36–W38.